

Information Quality Ratio as a novel metric for mother wavelet selection



Dedy Rahman Wijaya^{a,b,*}, Riyanarto Sarno^a, Enny Zulaika^c

^a Informatics Department, Institut Teknologi Sepuluh Nopember, Surabaya, Indonesia

^b School of Applied Science, Telkom University, Bandung, Indonesia

^c Biology Department, Institut Teknologi Sepuluh Nopember, Surabaya, Indonesia

ARTICLE INFO

Keywords:

Information Quality Ratio

Electronic nose

Wavelet transform

Mother wavelet selection

ABSTRACT

This study proposes Information Quality Ratio (IQR) as a new metric for mother wavelet selection in real-world applications. In mother wavelet selection, common metrics such as MSE and correlation coefficient highlight the morphological similarity as well as SNR focuses on enlarging signal power against noise power. Instead, IQR emphasizes that the reconstructed signal has to keep essential information from the original signal. Regarding mother wavelet selection problem, we also demonstrate the effect of wavelet transform at various decomposition levels to make a clear foundation of wavelet decomposition. In this study, IQR was used to determine the best-suited mother wavelet for electronic nose signals in beef quality classification. The experimental results show that IQR based mother wavelets have better capability to keep essential information from original signals than SNR, MSE, and correlation coefficient based mother wavelets. Moreover, it has better sensitivity to quantify the changes of signal structure than MSE and correlation coefficient.

1. Introduction

The wavelet transform is an excellent technique for non-stationary signal analysis. Actually, it provides both of time and frequency resolution for a particular signal in many real-world applications. Another advantage of the wavelet transform is the abundance of mother wavelet families. However, this advantage also inflicts question what is the most appropriate mother wavelet (MWT) family for particular signal? Basically, the main purpose of the wavelet transform is denoising and compressing a signal without losing the essential information and original signal characteristic. So, it is necessary to do an exhaustive analysis to find the most appropriate MWT for a particular signal and make sure the reconstructed signal still keep essential information.

In this study, we conduct an analysis of the beef quality classification based on electronic nose (e-nose) signals. E-nose is the example of a real-world application which generates signals from gas sensors. It is composed of several gas sensors which are called gas sensor array. They have a different selectivity of gasses and different signal characteristics. In many e-nose applications, several sensors with different selectivity are used for analytical or classification tasks such as milk quality identification [1,2], classification of tea or coffee [3,4], fish species identification (anchovy, horse mackerel, and whiting) [5], classification of saffron [6], fruit identification (durian, jackfruit, and mango) [7], and beef quality classification [8–14]. On the other hand, some studies attempt to solve sensor optimization problems for a particular applica-

tion. Commonly, feature selection and statistic technique are used to deal with sensor array optimization problem such as rough set-based [15], combinational feature selection [16], GA-statistical approach [17], etc. Furthermore, several studies attempt to compare data analysis techniques such as clustering technique [18] and classifier algorithm for e-nose dataset [19]. Another study attempts to define a signal model for e-nose though not perform model validation [20].

Basically, the signal generated by sensor array contains noise. It is caused by sensors interference, large heating current, power dissipation, etc. It was reported that the signal from gas sensors can contain 20% of noise in the severe condition [21]. According to the explanation above, the noise from a gas sensor cannot be ignored and it is very important to reduce the noise for computational efficiency and a more valid result of further analysis. It became essential when e-nose data analysis work on Sensing as a Service (S²aaS) environment [22]. Based on the previous explanation, this study has the following motivations:

- 1) Different applications have different signal characteristics. The best-suited MWT family needs to determine for each signal. Common metrics such as Mean Square Error (MSE) and correlation coefficient are only focused on a morphological similarity between original and reconstructed signals. In addition, Signal to Noise Ratio (SNR) focuses on how dominant signal power against noise power. Whereas, it is very important to determine the best-suited MWT with considering the information quality of the reconstructed signal to guarantee it still keeps essential information.

* Corresponding author at: School of Applied Science, Telkom University, Bandung, Indonesia.

- 2) We found that the level of wavelet decomposition has a great influence on the information of signal. However, many of the previous studies did not provide a clear foundation of appropriate decomposition level. It needs more exhaustive analysis to determine the decomposition level in wavelet transform.
- 3) There is no study on the best-suited MWT for e-nose application.

This paper proposes Information Quality Ratio (IQR) for MWT selection. Signals from 7 sensors are analyzed to find the best-suited MWT for the beef quality classification task. The experiment was conducted to observe the gasses produced by the decay of beef in 3 days. Furthermore, we also analyze the effect of wavelet decomposition level to a relationship with a class label of beef quality. It is also a caution to researchers and practitioners to determine the appropriate wavelet decomposition level for signal reconstruction.

The rest of this paper is organized into the following sections: [Section 2](#) provides an explanation of related works including e-nose for beef quality classification and MWT selection. [Section 3](#) illustrates how Discrete Wavelet Transform works. [Section 4](#) describes the proposed Information Quality Ratio (IQR) for MWT selection. [Section 5](#) explains the material and methods used in the experiment. [Section 6](#) describes results of the experiment including the effect of wavelet decomposition level, the best-suited MWT for the signals of e-nose on the beef quality classification task, and the performance comparison between IQR, MSE, correlation coefficient, and SNR. Finally, [Section 7](#) is the conclusion of this work.

2. Related works

Beef quality classification is one of popular area for e-nose utilization. Several studies attempt to differentiate the beef quality into two classes (unspoiled and spoiled) [10,11,14,23]. They successfully perform binary classification with more than 90% of prediction accuracy. In the last three years, e-nose combined with the particular pattern recognition techniques is used to solve three classes classification problem for beef quality classification (fresh, semi-fresh, and spoiled) [8,24,25]. Certainly, the performance of multiclass classification task is lower than binary classification (less than 90% accuracy). Because the multiclass classification is harder than binary classification problem [8,25]. Another work claims the higher performance though using few data testing [24]. The details about the studies of e-nose for beef quality

classification are demonstrated in [Table 1](#).

However, all of them did not refer to the Meat Standards Committee of ARMCANZ (Agricultural and Resource Management Council of Australia and New Zealand) which is described in [Table 4](#). According to this standard, the quality of meat is divided into four classes (excellent, good, acceptable, and spoiled) [26]. Definitely, distinguishing the meat into four classes is more difficult than two or three classes. Since more classes mean more boundaries between classes that lead to increased number of prediction errors. In binary classification, the probability of the correct classification is $1/2$, while in multiclass classification problem with m classes is $1/m$.

In preprocessing phase, most of the previous works directly employ PCA for feature extraction instead detailed discusses how to handle the noise. In fact, it was reported that the signal of gas sensor can contain 20% of noise in severe conditions [21]. Whereas, the presence of noise aggravates the accuracy, time in building, complexity of classifier, and weaken the detection limit of the instrumental technique [27,29]. These matters because the presence of noise can cause overlapping between classes in their boundaries [28]. The exhaustive analysis of noise impact in multiclass classification problem was reported. Employing noise reduction technique for data training and data testing is a promising solution for accuracy improvement [29]. Thus, performing noise reduction properly is very important especially in e-nose applications. Therefore, we have to deal with this problem in the multiclass classification task.

The wavelet transform is a common technique for non-stationary signal denoising. In e-nose studies, the wavelet transform is utilized for noise filtering. E-nose is a prospective instrument for wound infection detection in mice. Db1 mother wavelet with thirteen decomposition level is used to find the hidden information of wound infection. The approximate coefficient is extracted as hidden information of wound infection because it is buried the smell of the mice themselves. The approximate coefficient of wavelet transform presents the better result of classification accuracy than the original signal based on Radial Based Function Neural Network (RBFNN) [30]. Furthermore, wavelet transform has a lot of wavelet families e.g. haar, daubechies (db), symlet (sym), coiflet (coif), etc. Each of them can be subdivided into many variants. For instance, db wavelet has variants db1 to db10, sym wavelet has variants sym2 to sym15, and so on. The problem is how to determine the most appropriate MWT for a particular signal. [Table 2](#) shows the previous studies to determine the best-suited MWT for

Table 1
The studies of e-nose for beef quality classification.

No	Applications	Sensing Elements	The number of sensors	Preprocessing Techniques	Classification Techniques	The Number of Classes	Accuracy	Ref
1	Beef quality classification	Built-in Cyranose-320	28 gas sensors	Binomial smoothing, averaging, and normalization, Principal Component Analysis (PCA)	Linear discriminant analysis (LDA) and quadratic discriminant analysis (QDA)	Two classes (Unspoiled, Spoiled)	98.48% by QDA	[11]
2	Beef and sheep meat quality classification	Taguchi gas sensors (Figaro)	6 gas sensors + temperature & humidity sensor	Principal Component Analysis (PCA)	Support Vector Machine (SVM)	Two classes (Unspoiled, Spoiled)	98.81% for beef and 96.43% for sheep meat > 90%	[14]
3	Beef quality classification	A custom-built metal oxide-based e-nose	6 gas sensors + temperature & humidity sensor	Principal Component Analysis (PCA)	Radial Basis Function Neural Networks (RBFNN)	Two classes (Unspoiled, Spoiled)	> 90%	[10]
4	Beef and fish quality classification	A custom-built metal oxide-based e-nose	8 gas sensors	Moving average finite impulse response, steady state response	Artificial Neural Network, Support Vector Machine, and k-nearest neighbor	Two classes (Unspoiled, Spoiled)	96.2% by KNN	[23]
5	Beef quality classification	LibraNose, Technobio chip e-nose	8 gas sensors	Principal Component Analysis (PCA)	Support Vector Machine (SVM)	Three classes (fresh, semi-fresh, and spoiled)	89%	[8]
6	Beef quality classification	LibraNose, Technobio chip e-nose	8 gas sensors	Robust Principal Component Analysis (RPCA)	Fuzzy-Wavelet Neural Network (FWNN)	Three classes (fresh, semi-fresh, and spoiled)	97.14%	[24]
7	Beef quality classification	LibraNose, Techno biochip e-nose	8 gas sensors	–	Ensemble-based classifiers	Three classes (fresh, semi-fresh, and spoiled)	85%	[25]

Table 2
The MWT families in various applications.

No	Applications	Metrics	MWT	Decomposition level	Ref
1	Electrocardiogram (ECG) signal	Compression Ratio and Percent Root Mean Square Difference	db1	not explained	[31]
2	ECG signal which contaminated with White Gaussian Noise (WGN)	Mean square error (MSE), Signal to Noise Ratio (SNR), and correlation coefficient	db9	2 levels	[32]
3	Electroencephalography (EEG) Signals during Working Memory Task	Signal to Noise Ratio (SNR), Peak Signal to Noise Ratio (PSNR), Mean Square Error (MSE) and xcorr	sym9	4 levels	[33]
4	EEG Signals during Working Memory Task	xcorr combined with ANOVA	sym9	5 levels	[34]
5	EEG signal	PNN and SVM classification rate	coif1	6 levels	[35]
6	EEG signals for epileptic detection	k-Nearest Neighbor (k-NN) classification rate	dmey	3 levels	[36]
7	Biological signals: forearm EMG, EEG and vaginal pulse amplitude (VPA)	Segmentation of signals	db44	4 levels	[37]
8	Ultrasound image denoising	Peak Signal to Noise Ratio (PSNR) and edges preservation measure	orthogonal wavelet family	1–2 levels	[38]
9	Microemboli classification	SVM classification rate	db6	2 levels	[39]
10	Hydrologic forecasting	Mean absolute error (MAE), Root mean square error (RMSE), Nash-Sutcliffe criteria (NSC)	no universal MWT for all type of time series data	2–4 levels	[40]
11	Rainfall-runoff modeling	multilayer perceptron neural network (MLPNN) or radial basis function neural network (RBFNN) classification rate	db8	9 levels	[41]
12	Analyzing power system fault transients	waveform shape of the signal (orthonormality)	db4 for voltage signals while db5 for current signals	not explained	[42]
13	Infant cry classification	similarity (Cross-correlation), regularity (decomposed wavelet coefficients), and classification rate	dmey	5 levels	[43]
14	ECG signals contaminated by noise	energy, entropy, energy-to-entropy ratio, joint entropy, conditional entropy, mutual information, relative entropy	Each metric result different MWT	8 levels	[44]
15	Bearing vibration signals analysis	Energy-to-Shannon entropy ratio	complex Morlet	not explained	[45]

various signals denoising.

All of the previous works attempt to use several metrics to find the best MWT for particular applications. Common metrics such as MSE, SNR, PSNR, correlation coefficient, and classification rate were used. For example, the bigger SNR and PSNR mean to maximize the signal power against noise power to get the bigger ratio. The smaller MSE means the smaller error or differences between original and reconstructed signals. Correlation coefficient also quantifies the degree of linear relationship or similarity between two variables. Hence, MSE and correlation coefficient give almost similar results. Whereas, directly using classifiers for MWT selection cannot guarantee that the result is free from an overfitting issue. Furthermore, most of the previous studies lack analyzes the effect of the decomposition level in the MWT selection. We only find three works which analyzing classification accuracy with different level of decomposition [35] and comparing the performance of 6 MWT in different decomposition level based on RMSE, MAE, and NSC [40]. Another work proposes cross-validation (CV) to determine MWT and the best decomposition level though it does not provide further discussion about the analysis of decomposition effect [27]. It also states that the proper decomposition level is more important than MWT in several cases. Hence, it is very important to properly determine the decomposition level before performing MWT selection because the metrics will generate different results at the different level of decomposition. It became caution for researchers and practitioners to be more careful to determine the level of wavelet decomposition.

Based on the explanation above, we give a different view of MWT selection. This paper proposed a new metric based on information-theoretic to determine the best-suited MWT. This metric guarantee that reconstructed signal can keep essential information from the original signal. In this study, we attempt to find the best-suited MWT of each signal generated by gas sensor array. In the experiment, e-nose used to detect beef spoilage based on gasses that produced by mesophilic bacteria. Furthermore, we also demonstrate the effect of wavelet transform for the correlation between signals and class label at the different level of decomposition.

3. Discrete wavelet transform

Discrete wavelet transform (DWT) is a popular technique for time-frequency resolution of time series data by decomposing the non-stationary signal into a 2D, time-frequency domain. Wavelet transform of a signal $x(t)$ can be expressed in the Eq. (1) as follows [46]:

$$wt(s, \varphi) = \langle x, \omega_{s,\varphi} \rangle = \frac{1}{\sqrt{s}} \int_{-\infty}^{\infty} x(t) \omega^* \left(\frac{t-\varphi}{s} \right) dt \tag{1}$$

Wherein the s symbol represents the scaling parameter of the base wavelet $\left(\frac{t-\varphi}{s}\right)$. Then $\omega^*(\cdot)$ denotes complex conjugation of the base wavelet. The φ is a parameter that translates wavelet shifting the time axis. The ω symbol describes the base wavelet is used. Performing DWT has some advantage than Continuous Wavelet Transform (CWT), such as reducing computational time and memory size. DWT uses discrete value for scaling and translation parameters as follows:

$$dwt(s, \varphi) \begin{cases} s = s_0^i \\ s_0 < 1, \varphi_0 \neq 0, k \in Z \\ \varphi = k\varphi_0 s^i \end{cases}$$

Commonly, $s_0=2$ and $\varphi_0=1$ so the DWT of signal $x(t)$ is expressed in the following Eq. (2):

$$dwt(i, k) = \langle x(t), \omega_{i,k}(t) \rangle = \frac{1}{\sqrt{2^i}} \int_{-\infty}^{\infty} x(t) \omega^* \left(\frac{t - k2^i}{2^i} \right) dt \tag{2}$$

There are several types of common used MWTs such as haar, daubechies, coiflet, symlet, biorthogonal, reverse biorthogonal, and meyer wavelet. In general, DWT is used for noise filtering. The signal contaminated with noise can be expressed in Eq. (3) as follows:

$$x(t) = y(t) + \theta * n(t) \tag{3}$$

While $x(t), y(t), n(t), \theta$ are signal contaminated with noise, reconstructed signal, noise, and noise level, respectively. Basically, the main purpose of signal denoising is to reduce θ and keep $y(t)$. Basically, it has three steps: signal decomposition, coefficients thresholding, and signal reconstruction [46]. Fig. 1 shows an example of the signal e-nose with the three levels of decomposition.

At first level, an original signal is processed by the high-pass and

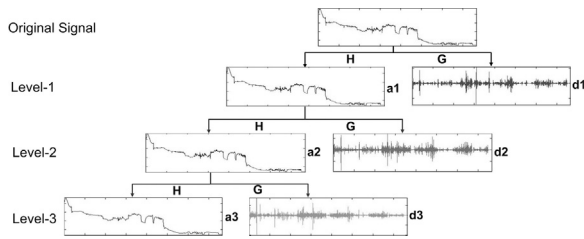


Fig. 1. Three level decomposition of e-nose signal using DWT. H is low pass filter, G is high pass filter, A is approximate coefficients, and D is detailed coefficients.

low-pass filter. The result of the high-pass filter is detailed coefficient ($d1$) and the result of the low-pass filter is approximate coefficient ($a1$). Later, $a1$ is filtered again and this process is repeated until three times of decomposition. The final result is approximate coefficient ($a3$) and the entire detail coefficient ($d1, d2, d3$). Hence, $y(t)$ as reconstructed signal can be expressed in the following Eq. (4):

$$y(t)=a3 + d3 + d2 + d1 \tag{4}$$

The question is how good DWT can reduce the noise level (θ) and reconstruct a signal without losing the essential information? Inappropriate MWT and decomposition level lead to the signal defect and losing of essential information.

4. Proposed Information Quality Ratio

In this work, we proposed a metric based on information-theoretic which is called information quality ratio (IQR) to determine the best-suited MWT. Based on the concept of information theory, the mutual dependence between two variables can be measured by mutual information (MI). It quantifies the amount of information of a variable based on another variable in bits unit. If $x(t), y(t)$ are original and reconstructed signal respectively then the schematic relationship between them can be described in Fig. 2.

According to Fig. 2, the whole set is represented by joint entropy $H(\{x(t), y(t)\})$. The joint entropy between $x(t)$ and $y(t)$ with joint mass probability $p(x_i, y_j)$ is a total of uncertainty contained in two signals. Mathematically, it can be expressed with the following Eq. (5):

$$H(\{x(t), y(t)\})=- \sum_{x_i \in x(t)} \sum_{y_j \in y(t)} p(x_i, y_j) \log_2(p(x_i, y_j)) \tag{5}$$

While mutual information quantifies how good DWT with particular MWT can reconstruct original signal ($x(t)$). The mutual information between original signal ($x(t)$) and reconstructed signal ($y(t)$) can be expressed by following Eq. (6):

$$I(x(t); y(t))= \sum_{x_i \in x(t)} \sum_{y_j \in y(t)} p(x_i, y_j) \log_2 \left(\frac{p(x_i, y_j)}{p(x_i)p(y_j)} \right) \tag{6}$$

It can be interpreted that the greater mutual information between original and reconstructed signal means DWT with particular MWT has better capability to reconstruct a signal with minimizing information loss. However, the value of mutual information cannot be compared directly with others without considering the total uncertainty. Considering a fair comparison, it needs to be normalized. Hence, the value of mutual information between two signals has to be divided by total uncertainty to yield ratio or percentage. In MWT selection problem, the best-suited MWT can be determined by quantifying this ratio. The biggest ratio means the reconstructed signal is preferable to keep essential information. The IQR of original signal ($x(t)$) and reconstructed signal ($y(t)$) can be expressed as expected value of mutual information in Eq. (7):

$$IQR(x(t), y(t)) = E_{x(t), y(t)}[I(x(t); y(t))] = \frac{I(x(t); y(t))}{H(\{x(t), y(t)\})} \tag{7}$$

Finally, according to the equation above, it can be simplified in Eq. (8) as follows:

$$IQR(x(t), y(t)) = \frac{\sum_{x_i \in x(t)} \sum_{y_j \in y(t)} p(x_i, y_j) \log_2(p(x_i)p(y_j))}{\sum_{x_i \in x(t)} \sum_{y_j \in y(t)} p(x_i, y_j) \log_2(p(x_i, y_j))} - 1 \tag{8}$$

Where x_i and y_j are particular value of $x(t)$ and $y(t)$ respectively. $p(x_i)$ and $p(y_j)$ are the marginal probability and $P(x_i, y_j)$ is joint probability of x_i and y_j . Naturally, the range of IQR is [0,1]. The biggest value ($IQR = 1$) can be reached if DWT can perfectly reconstruct a signal without losing of information. Otherwise, the lowest value ($IQR = 0$) means MWT is not compatible with an original signal. In the other words, a reconstructed signal with particular MWT cannot keep essential information and totally different with original signal characteristics. Therefore, IQR has the following properties: non-negative, non-linear, and normalized.

According to Eq. (8), the comparison of m different mother wavelet can be expressed with the following vector v :

$$v=[IQR_1 \quad IQR_2 \quad \dots \quad IQR_m]$$

The best-suited MWT can be determined by the maximum value of IQR in vector v which is expressed in Eq. (9):

$$IQR_{best-v} = \max(v) \tag{9}$$

In sensor array signal processing, each signal can have the most suitable MWT. If we have n sensors in sensor array then it can be expressed in the following $R_{n \times m}$ matrix:

$$R_{n \times m} = \begin{bmatrix} IQR_{11} & \dots & IQR_{1m} \\ \vdots & \ddots & \vdots \\ IQR_{n1} & \dots & IQR_{nm} \end{bmatrix}$$

So, the best-suited MWT of each sensor in a sensor array according to the above matrix can be expressed in Eq. (10) as follows:

$$\begin{bmatrix} IQR_{best-1} \\ \vdots \\ IQR_{best-n} \end{bmatrix} = \begin{bmatrix} \max(IQR_{1\dots}) \\ \vdots \\ \max(IQR_{n\dots}) \end{bmatrix} \tag{10}$$

5. Materials and methods

5.1. Materials

A gas sensor array with the various gas sensor is used to detect gasses from beef spoilage which produced by mesophilic bacteria. A gas sensor array that consists of various gas sensors is used to detect gasses of beef spoilage. Mesophilic bacteria grow optimally at moderate temperature (20° to 45 °C). In this condition, *Pseudomonas sp* is the

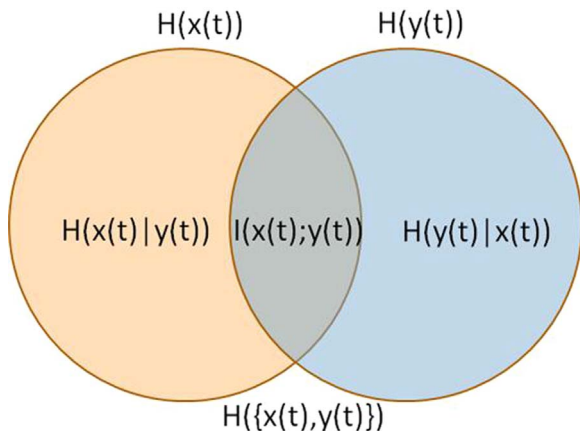


Fig. 2. Venn diagram of various information measures: $x(t)$ is original signal and $y(t)$ is reconstructed signal.

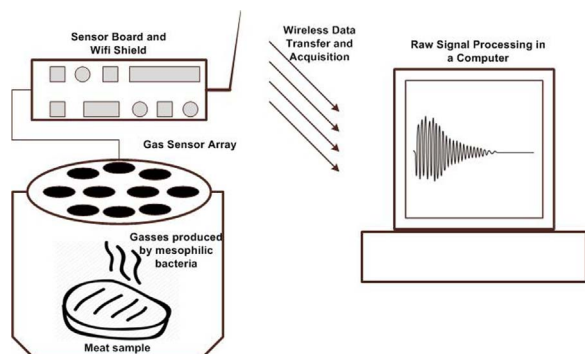


Fig. 3. Schematic experiment of beef spoilage observation using Electronic Nose.

most dominant bacteria on aerobically stored meat due to the ability of the bacterium to use amino acid (creatine and creatinine) to growth [47]. The Arduino microcontroller performs Analog to Digital Conversion and transfers data which is generated by each gas sensor via a wireless network to the computer. The illustration of the experimental scheme can be seen in Fig. 3.

In an initial experiment, we use eleven sensors consist of ten gas sensors and one temperature and humidity sensor. The selectivity of each gas sensor in initial sensor array can be seen in Table 3.

Experimental data is collected with a minute of sampling rate in about 60 h to observe gasses yielded by beef spoilage. The raw signals from 11 gas sensors are shown in Fig. 4.

In this study, the grade of beef is based on standard issued by Meat Standards Committee of ARMCANZ (Agricultural and Resource Management Council of Australia and New Zealand). It uses amount of bacterial cells in *cfu/g* unit on meat that shown in Table 4 as follows:

According to Table 4, the spoilage of beef can be precisely determined. Therefore, Fig. 5 demonstrates the real bacterial growth in the aerobic environment. Spectrophotometer (Genesys 20) is used to measure optical density (600 nm) and hemocytometer is used to calculate the number of cells. The experiment adopts classical and two-hour methods [48]. It also demonstrates the history of the meat quality (excellent, good, acceptable, and spoiled).

According to the curve area in Fig. 5 and the signals of e-nose, we construct a feature set in the following tuple tp which is expressed in Eq. (11):

$$tp = \langle \min, x_1, x_2, \dots, x_k, class \rangle \quad (11)$$

\min is the time when a particular tuple is generated (in minutes). x is the signals from the gas sensor array. k is sensor amount in the sensor array, and $class$ is class label based on bacterial population.

5.2. Experimental setup

The beef sample placed on the sensor box. The aims are the gasses can be easily collected and detected by the sensor array. If the sample is

Table 3
Initial gas sensors list in the sensor array.

No	Sensor	Selectivity
1	MQ135	NH ₃ (Ammonia), NO _x , alcohol, Benzene, smoke, CO ₂
2	MQ136	Hydrogen Sulfide (H ₂ S)
3	MQ2	LPG, i-butane, propane, methane, alcohol, Hydrogen, smoke
4	MQ3	Alcohol, Benzene, Methane (CH ₄), Hexane, LPG, CO
5	MQ4	Methane (CH ₄), Natural gas
6	MQ5	LPG, natural gas, town gas
7	MQ6	LPG, iso-butane, propane
8	MQ7	Carbon Monoxide (CO)
9	MQ8	Hydrogen (H ₂)
10	MQ9	Methane, Propane and CO
11	DHT22	Temperature & Humidity

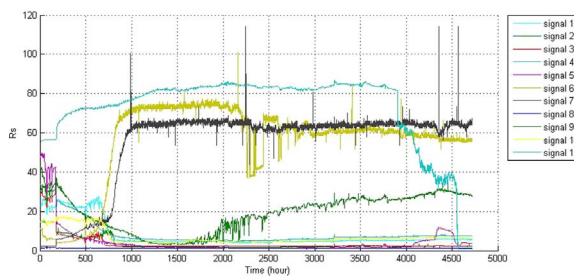


Fig. 4. Original signals of gas sensor array.

Table 4
Class of beef quality.

Category	Amount of Bacterial Cells (log ₁₀ cfu/g)
Excellent	< 3
Good	3–4
Acceptable	4–5
Spoiled	> 5

*cfu/g: colony forming unit of bacteria in 1 g of beef.

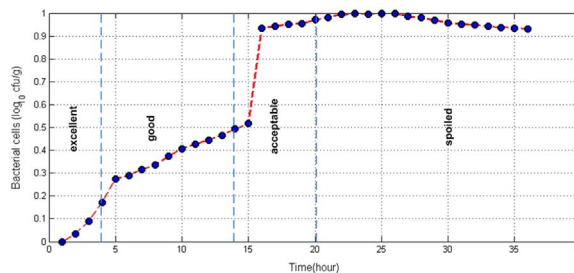


Fig. 5. Bacterial growth and class of beef quality at room temperature [49].

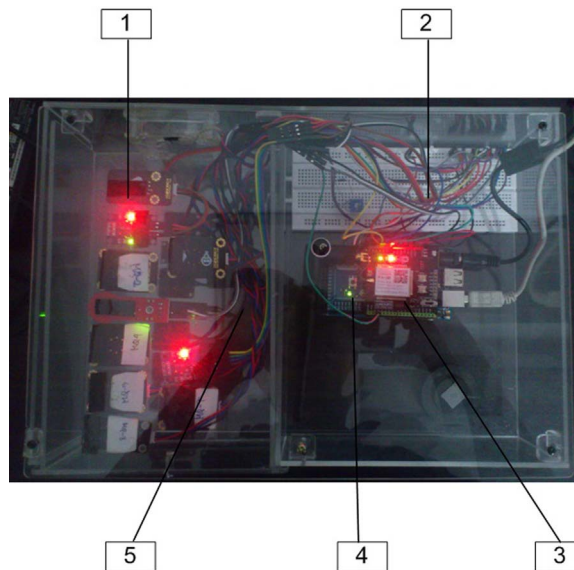


Fig. 6. Experimental environment: (1) Sensor array (2) Project board (3) Wifi-shield (4) Arduino microcontroller (5) Beef sample.

placed on the open space then it will lead to the spread of gasses. It can cause instability of sensor responses which generates more noisy data. Fig. 6 shows the experimental environment using custom electronic nose sensor box.

In fact, water vapor is one of the results from the beef spoilage. The presence of water vapor causes changes in humidity level. Commonly,

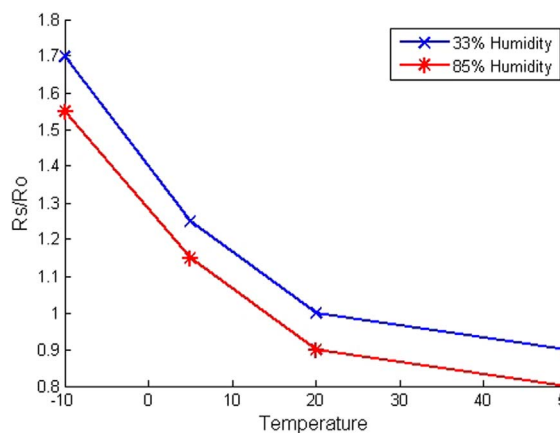


Fig. 7. Typical dependence of the gas sensor response on temperature and humidity.

Meta-Oxide Semiconductor (MOS) gas sensor uses Tin Dioxide (SnO_2) as sensing material. The response of gas sensor can be affected by the condition of the environment such as temperature and humidity [50]. Using the sensor in standard environmental conditions will ensure that it produces a normal response. According to the gas sensor datasheets, Fig. 7 shows the relationship between the gas sensor and environmental condition.

Fig. 7 demonstrates the optimal working environment (temperature and humidity) of the gas sensors used in this experiment. It shows that the optimum humidity level is in the range between 33% and 85% although the sensor datasheet allows up to 95% of relative humidity. Furthermore, the range of operational temperature is between -10° and 50°C . The DHT22 sensor is employed to record temperature and humidity levels in the sampling room to ensure the experiment is still in the appropriate condition. Fig. 8 shows the environmental condition related to the temperature and humidity levels.

The temperature levels in this experiment are between 33.5 and 39.9. So, there is no issue related to the temperature. According to Fig. 8, the minimum humidity level is 55.1 in the first three minutes. Furthermore, the maximum humidity level is 86.8. It is a little bit higher than standard working humidity but it only occur during 9 minutes and there are no significant effects on the sensor responses.

In the experiment, 38 MWTs were compared such as daubechies (db1-db10), symlet (sym2-sym8), coiflet (coif1-coif5), biorthogonal (bior1.1, bior1.3, bior1.5, bior2.2, bior2.4, bior2.6, bior2.8, bior3.1,

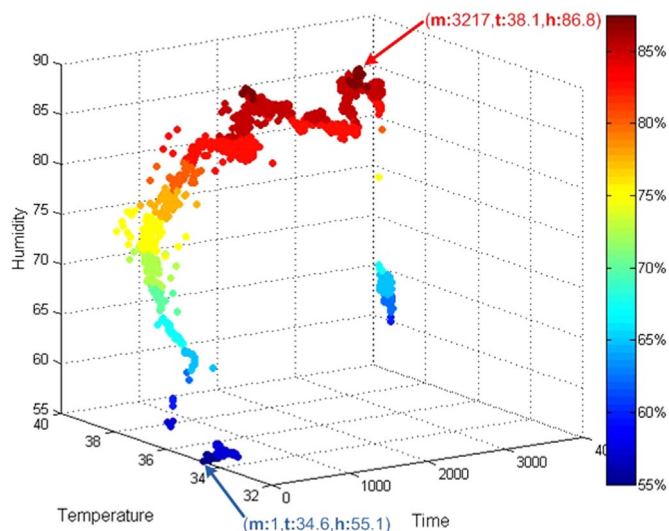


Fig. 8. Temperature and humidity levels in the experiment: m , t , and h are time, temperature, and humidity level, respectively.

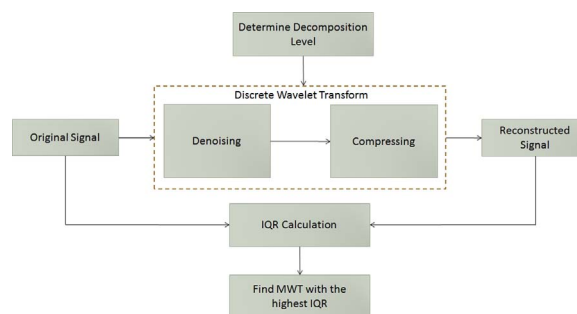


Fig. 9. MWT selection procedure based on IQR.

bior3.3, bior3.5, bior3.7, bior3.9, bior4.4, bior5.5, bior6.8), and dmev. The IQR values are calculated between original and reconstructed signal using modified version of MIToolbox for C and MATLAB [51]. Fig. 9 shows a procedure how to calculate IQR to find the most appropriate MWT.

The first step is determining decomposition level of each signal. It can be determined by the predominant frequency of each signal. Then the second step, original noisy signals are denoised and compressed to yield reconstructed signals. The third step, a gap between original and reconstructed signal is quantified by IQR. The last step, the best-suited MWT can be determined by the highest IQR.

6. Results and discussion

Based on the experimental procedure, there are two main results of this work. First, we observe the effect of wavelet decomposition level against the relationship between reconstructed signals and class label. It becomes caution for practitioners and researchers to perform DWT with proper decomposition level. Second, we demonstrate MWT selection based on IQR to find the best-suited MWT for the gas sensor signals in the beef quality classification. Previously, we perform a sensor array optimization (sensors selection) to determine the best sensors combination.

6.1. Sensor array optimization

Sensor array optimization is an essential step to finding the most optimal combination of the gas sensor array in many e-nose applications. Basically, a sensor array combination has two issues. First, sensors are irrelevant with the target sample. Second, they contain an overlapping selectivity among sensors with others. Resolving the sensor array optimization problem has several advantages such as improvement of the classifier accuracy, increasing the speed of the algorithm, minimizing the computation resources, overlapping selectivity reduction, energy saving, and network data traffic reduction for online analysis. Actually, sensor array optimization problem associates with feature selection problem. The selected feature represents the best sensor combination for a particular application. There are popular feature selection techniques such as wrapper, embedded, and filter. Further, filter technique has promising advantages such as independent of the classifier, robustness against the overfitting problem, and relatively fast than others [52,53]. In this research, modified Fast Correlation-Based Filter (FCBF) is used to determine features associated with the combination of sensors in the sensor array. The performance of FCBF for a large number of feature reduction and an accuracy improvement of the classifier was reported [54,55]. Fig. 10 shows the complete procedure of sensor array optimization.

6.1.1. Signal processing

Signal processing is a fundamental step in sensor array optimization. The characteristic of the raw signal is identified to determine the appropriate way for signal treatment. Basically, signals are widely

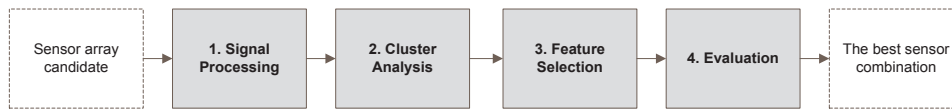


Fig. 10. Sensor array optimization steps [49].

classified as deterministic and non-deterministic (random signal) [46]. The deterministic means the signal can be modeled mathematically and vice versa. The deterministic signal can be divided into periodic and transient. On the other hand, the non-deterministic signal can be classified into stationary and non-stationary (random). Based on in Fig. 4, the raw signals are very difficult to be expressed mathematically. Hence, the assumption that the raw signals are deterministic is not safe. Furthermore, we also tested the sample of the raw signal to know whether the signal is stationary or non-stationary. Kwiatkowski Phillips Schmidt Shin (KPSS) test is employed to show the specific characteristic of the raw signal. The KPSS test is used to prove one of the two hypotheses. First, null hypothesis (H_0) means the series is stationary. Second, alternative hypothesis (H_a) means the series is non-stationary. Besides, the characteristic of the signal can be known by using KPSS test which is expressed in Eq. (12) as follows [56]:

$$S_{char} = \sum_{k=1}^N \frac{x(k)^2}{x_{nw}^2 N^2} \tag{12}$$

Where N is the length of the signal, $x(k)$ is the total of vector of residual from regression. x_{nw}^2 is the Newey-West estimator of the long-run variance. The results of KPSS test show that all of gas sensor signals are non-stationary with risk to reject H_0 is $< 0.01\%$. It means all of signals are non-stationary. Aforementioned, the wavelet transform is an excellent technique for non-stationary signal analysis. In this work, DWT is used for signal denoising and compressing.

6.1.2. Cluster analysis

Cluster analysis is needed to find the amount of clusters which associate with the maximum number of best features in feature selection algorithm. In this work, Agglomerative Hierarchical Clustering (AHC) is employed for cluster analysis. Centroid method with Euclidean distance is used because of the consistent performance for outlier data handling [57]. According to AHC result, the dendrogram in Fig. 11 shows the five groups of sensor in the sensor array. It shows that the combination of sensor in sensor array is roughly divided into 3 sensors group, 4 sensors group, 5 sensors group, 7 sensors group, or 8 sensors group.

6.1.3. Feature selection

Modified FCBF algorithm is used to find the optimum combination of k sensors in each sensor group. The optimum combination means minimizing redundant feature and eliminating irrelevant feature. It can

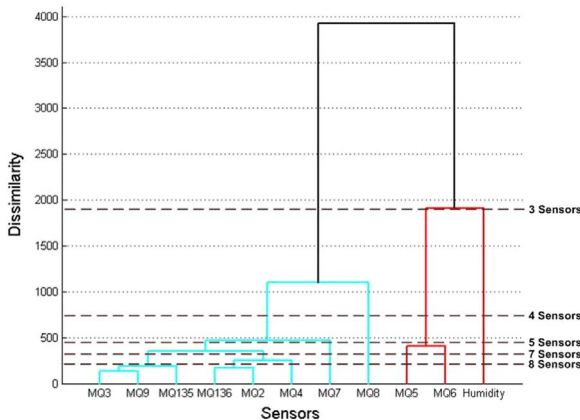


Fig. 11. The number of sensors in sensor array based on AHC result [49].

be obtained by modified FCBF algorithm and Symmetrical Uncertainty Matrix (SUM). Algorithm 1 demonstrates the modified FCBF algorithm which used in this work [49].

Algorithm 1. Modified FCBF Algorithm.

```

th ← 0.1 /* set SU minimum threshold*/
total_feature ← 11 /* the amount of the total features*/
/* Generating Symmetrical Uncertainty Matrix (SUM)*/
for i: 1 to total_feature+1 do
  for j: 1 total_feature+1 do
    tempval ← calculateSU(fi, fj)
    if (tempval ≤ th) then
      tempval ← 0
    end if
    SU(i, j) ← tempval
  end for
end for
/* Ranking the features*/
c_corr ← sort(c_correlation, 'descending')
k ← 7 /* setting the amount of the expected features*/
feature ← total_feature
/* Determining the best k features*/
i ← 1;
while (i ≤ total_feature-1) && (feature ≠ k) do
  j ← 1;
  while (j ≤ max_feature-1) do
    if (SU[i, total_feature+1-j] ≥ c_corr[total_feature+1-j]) then
      setInvalid(c_corr[total_feature+1-j])
      feature ← feature-1
      if (feature = k) then
        break
      end if
    end if
    j ← j+1
  end while
  i ← i+1
end while
  
```

According to SUM and Algorithm 1, Table 5 shows the gas sensor members in each sensor group (sub-array).

6.1.4. Evaluation

The main objective of evaluation step is to determine the best group of sensors. In the past works, two common ways are used to evaluate the quality of sub-array such as the classification rate [16,58,59] and distance measure [15,17,60]. The utilization of classification rate as an

Table 5
Sensor members in each sub-array [49].

Sensors group	Sensor group members
3 Sensors	MQ2, MQ135, MQ6
4 Sensors	MQ2, MQ135, MQ6, DHT22
5 Sensors	MQ2, MQ135, MQ6, DHT22, MQ4
7 Sensors	MQ2, MQ135, MQ6, DHT22, MQ4, MQ136, MQ9
8 Sensors	MQ2, MQ135, MQ6, DHT22, MQ4, MQ136, MQ9, MQ3

Table 6
The GRF value of each sub-array [49].

Sensors group	GRF value
3 Sensors	0.09101
4 Sensors	0.24844
5 Sensors	0.24298
7 Sensors	0.25005
8 Sensors	0.24882
All (11) Sensors	0.21592

Table 7
Wavelet decomposition level of 7 sensors [49].

Signal	Max frequency (Hz)	Decomposition level
1	0.43	11
2	0.43	11
3	0.43	11
5	0.65	10
7	0.43	11
10	0.65	10
11	0.65	10

evaluator not only depends on the quality of input feature but also affected by parameter settings and configurations of the particular classifier. So, using the classifier for evaluation does not guarantee the quality of input feature. According to the reason, this work uses General Resolution Factor (GRF) to evaluate the group of sensors [17]. GRF can be expressed by Eq. (13) as follows:

$$GRF = \sqrt{\sum_{i=1}^m \frac{(\mu_{i1} - \mu_{i2})^2}{\sigma_{i1}^2 + \sigma_{i2}^2}} \tag{13}$$

A larger probability of correct classification rate is associated with the larger ratio between centroid distance ($\sqrt{(\mu_{i1} - \mu_{i2})^2}$) and $\sqrt{\sigma_{i1}^2 + \sigma_{i2}^2}$. GRF values are calculated based on two first Principal Components (PCs) from Principal Component Analysis (PCA). All of GRF value of sub-arrays can be seen in Table 6.

Table 6 shows that 7 sensors group has the highest GRF than others. It presents 16% of the quality improvement than using all sensors. The higher GRF value is associated with the higher classification rate [17].

According to the sensor array optimization procedure before, this work uses 7 sensors group for beef quality detection which is associated with 7 signals (signal 1, signal 2, signal 3, signal 5, signal 7, signal 10, and signal 11). For more details, the sensor array optimization processes are explained in [49].

6.2. The effect of wavelet decomposition level

Basically, signal denoising is affecting the relationship between signal and the class label of beef quality. In this experiment, we exhibit the effect of wavelet decomposition level to the dependency between reconstructed signal and the class label. This dependency is called *C-correlation* [55] which measures the relationship between signal (x) and class in tuple tp . *C-correlation* is calculated by Symmetrical Uncertainty (SU). Furthermore, the rule to determine decomposition level can be expressed in Eq. (14) as follows [46]:

$$\frac{F_q}{2^{L+1}} \leq F_{char} \leq \frac{F_q}{2^L} \tag{14}$$

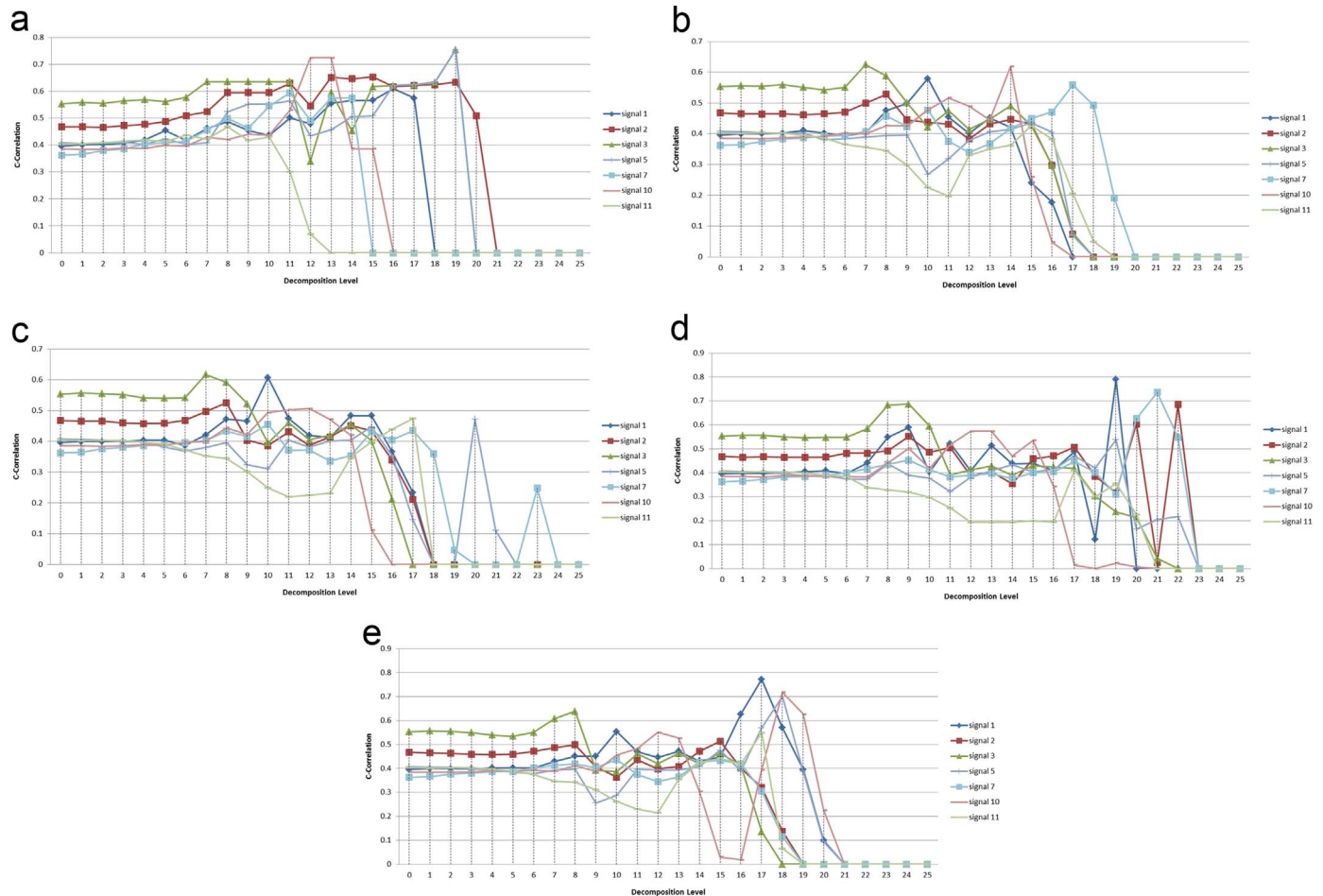


Fig. 12. The effect of wavelet decomposition level to *C-correlation* which is tested in several MWT families: Daubechies (a), Symlet (b), Coiflet (c), Biorthogonal (d), and Dmey (e).

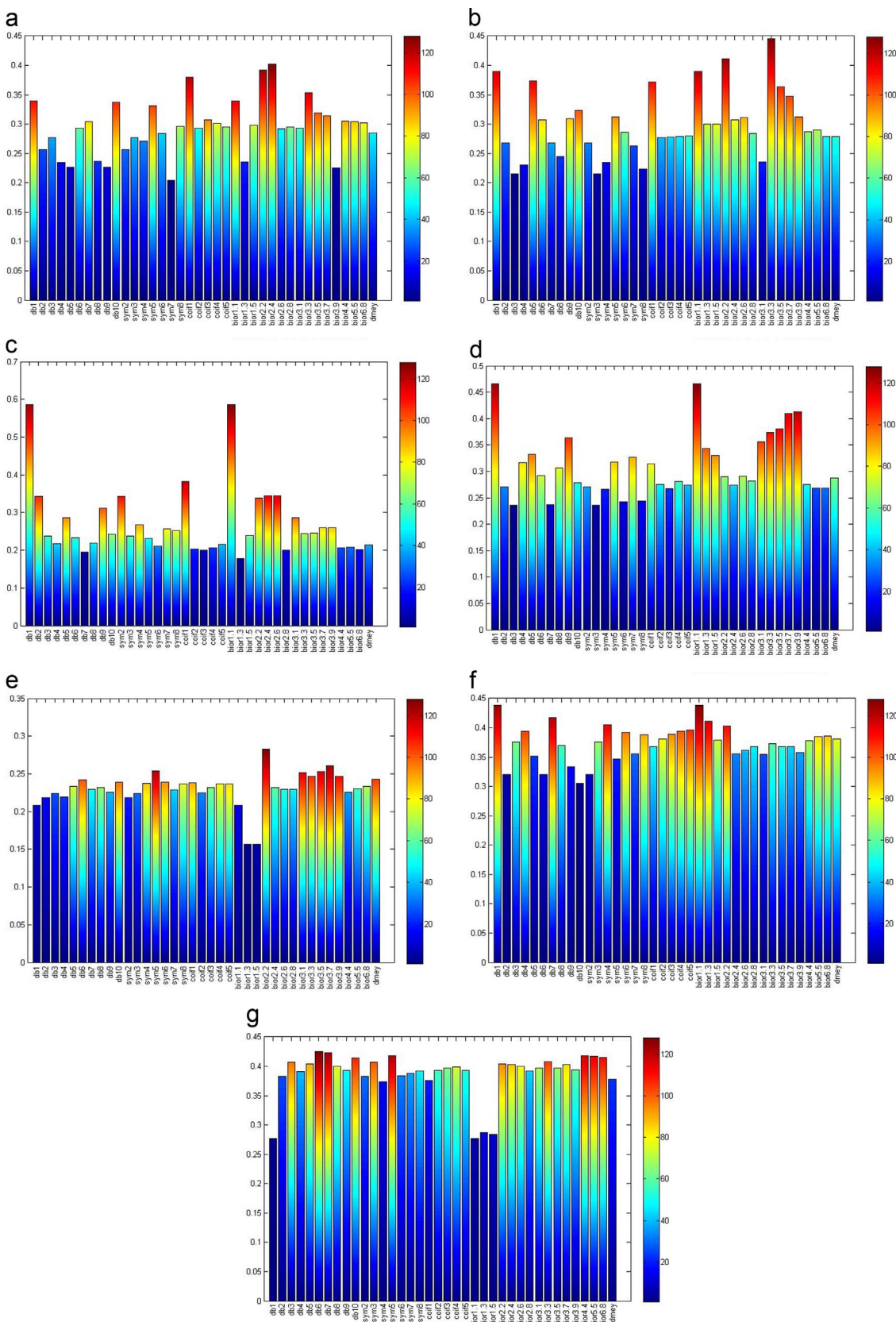


Fig. 13. IQR values of 38 MWTs in particular signals: signal 1 (a), signal 2 (b), signal 3 (c), signal 5 (d), signal 7 (e), signal 10 (f), signal 11 (g).

Where F_q , F_{char} , L are the sampling frequency, dominant frequency, and decomposition level, respectively. According to this rule, appropriate decomposition level with the sampling frequency (f_s) = 1024 Hz

can be seen in Table 7.

Table 7 shows the signals from 7 gas sensors should be decomposed to 10–11 level. We find that carelessly determine the decomposition

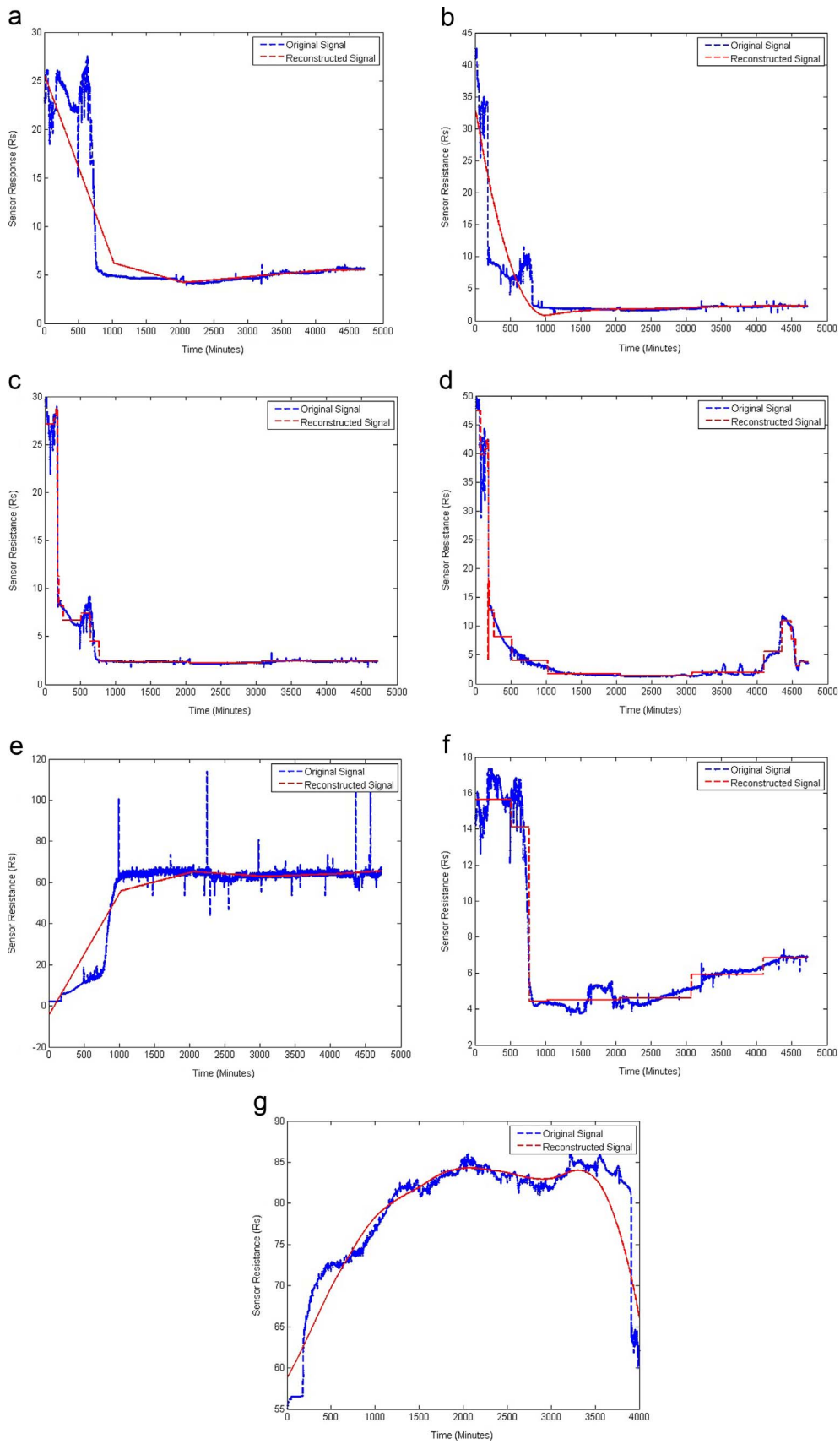


Fig. 14. The Original and reconstructed signals regarding with the best-suited MWT: signal 1 is reconstructed by bior2.4 (a), signal 2 is reconstructed by bior3.3 (b), signal 3 is reconstructed by db1 (c), signal 5 is reconstructed by db1 (d), signal 7 is reconstructed by bior2.2 (e), signal 10 is reconstructed by db1 (f), signal 11 is reconstructed by db6 (g) [49].

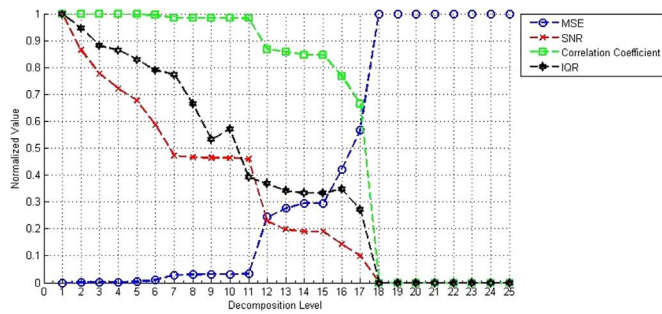


Fig. 15. The performance comparison of IQR, MSE, SNR, and Correlation Coefficient to quantify the changes of signal structure.

level can be lead to misleading of MWT selection result. Further, there is necessary to conduct further analysis the effect of decomposition level against *C-correlation*. Fig. 12 demonstrates the effect of wavelet transform to *C-correlation* in various decomposition levels.

In Eq. (1), scaling parameter (*s*) is associated with wavelet decomposition level. In Eq. (2), *s* is substituted by 2^i for discrete wavelet transform. The value of *i* represents the level of decomposition. The higher value of *i* means the lower frequency of a reconstructed signal. In the other words, a signal with low frequency requires a higher level of decomposition. Normally, noise filtering can improve *C-correlation* because it eliminates irrelevant data. However, it should be noted that performing too low decomposition level will cause not optimal denoising. In Fig. 12, zero decomposition level equals to an original signal. Commonly, there are no significant improvements of *C-correlation* at the low level of decomposition (lower than 10 levels) because of the higher morphological similarity with the original signal. Otherwise, assigning too high the level of decomposition will cause a signal distortion because of original signal characteristics loss. Fig. 12(a–e) shows that all of the wavelet families cannot present consistent result in the high level of decomposition (higher than 11 levels). While one signal has high *C-correlation* improvement, the other signal gets zero *C-correlation*. Finally, the entire *C-correlation* is equal to zero at the 24th level. It means improper wavelet decomposition can cause signal defect and loss of the essential information from the original signal. In addition, most of previous studies use one type of MWT for all signals. This is not entirely true because the results of our experiments show that the single MWT cannot be generalized for all signals.

6.3. MWT selection based on IQR

MWT selection is performed in MATLAB environment. The signals from gas sensor array are reconstructed by 38 MWT families with certain decomposition level according to the Table 7. The IQRs are calculated to quantify the amount of information which can be obtained by reconstructed signals from original signals. Then, they are compared to find the highest IQR value. Fig. 13 shows the IQRs comparison

among 38 MWTs on 7 signals that are generated by the sensor array.

Fig. 13 shows that each signal has the different best-suited MWT. Signal 1,2,3,5,7,10, and 11 compatible with bior2.4, bior3.3, db1, db1, bior2.2, db1, and db6, respectively. Moreover, Fig. 14 exhibits the comparison between reconstructed and original signals based on selected MWTs. Further, we also attempt to determine the best-suited MWT for signal 8 which has zero *C-correlation* at each level of decomposition. Actually, signal 8 represents carbon monoxide that has no relationship with beef spoilage. However, all of these MWTs are not compatible with signal 8 because all of the reconstructed signals have no mutual information with signal 8. It means noise reduction and compression will make severe defect and loss of essential information so signal 8 cannot be reconstructed.

6.4. Performance comparison between IQR, Mean Square Error (MSE), correlation coefficient, and Signal to Noise Ratio (SNR)

Definitely, wavelet decomposition inflicts the changes in the signal structure. The structural changes are in line with the decomposition level. If the structure of signal is changed then the metrics must be able to measure it. The question is how sensitive a particular metric can measure the changes. Fig. 15 demonstrates the performance of IQR against MSE, SNR, and correlation coefficient based on haar/db1 wavelet decomposition.

In Fig. 15, the values of MSE and correlation coefficient have no significant changes at 1st to 11th level of decomposition level but significantly changed after that. Otherwise, IQR and SNR progressively showing the signal structure changes at each level of decomposition. Finally, all of the metrics show that reconstructed signal is totally different than the original signal at level 18. According to Fig. 15, it can be said that IQR and SNR have better sensitivity to quantify the changes of signal structure than MSE and correlation coefficient. While SNR focuses on enlarging signal against noise power, IQR emphasizes how well DWT with a particular MWT can reconstruct original signal without losing essential information.

Table 8 shows that IQR based MWTs have better performance to filter the noise than correlation coefficient and MSE based MWTs. It is because of correlation coefficient and MSE more focus on morphological similarity rather than noise reduction. The orientation of correlation coefficient and MSE is the reconstructed signal should be similar with the original signal. It is problematic because signal denoising will definitely not optimal. On the contrary, SNR based MWTs are the best MWTs for signal denoising. However, according to the Table 9, they have the lowest performance to keep essential information from the original signals. It is because SNR focuses on enlarging the signal power against the noise power without considering information factor. Hence, IQR is a promising metric for MWT selection problem. It can determine the best MWT for the proper signal denoising.

Table 8

The comparison of noise reduction among the best-suited MWTs based on IQR, MSE, SNR, and Correlation Coefficient (P_{signal} and P_{noise} are the power of signal and noise, respectively).

Signals	IQR				SNR				Correlation Coefficient				MSE			
	MWT	P_{signal}	P_{noise}	%	MWT	P_{signal}	P_{noise}	%	MWT	P_{signal}	P_{noise}	%	MWT	P_{signal}	P_{noise}	%
1	bior2.4	81.94	6.44	7.86	bior3.1	104.20	2.36	2.26	db1	102.26	1.46	1.42	db1	102.26	1.46	1.42
2	bior3.3	41.24	8.33	20.21	bior2.8	106.06	41.32	38.96	db1	57.27	0.59	1.02	db1	57.27	0.59	1.02
3	db1	38.38	0.40	1.05	bior2.8	59.91	21.40	35.72	db1	38.38	0.40	1.05	db1	38.38	0.40	1.05
5	db1	86.15	1.08	1.25	bior4.4	107.36	28.25	26.32	db1	86.15	1.08	1.25	db1	86.15	1.08	1.25
7	bior2.2	3345.79	43.49	1.30	bior3.1	3413.19	44.66	1.31	bior2.2	3345.79	43.49	1.30	bior2.2	3345.79	43.49	1.30
10	db1	61.17	0.62	1.02	bior3.1	71.22	3.42	4.81	db1	61.17	0.62	1.02	db1	61.17	0.62	1.02
11	db6	5552.90	19.65	0.35	bior3.1	5725.22	39.68	0.69	db6	5552.90	19.65	0.35	db10	5547.24	17.42	0.31
Average				4.72				15.72				1.06				1.05

Table 9

The comparison of capability to keep essential information among the best-suited MWTs based on IQR, MSE, SNR, and Correlation Coefficient (MI and JE are mutual information and joint entropy, respectively).

Signals	IQR				SNR				Correlation Coefficient				MSE			
	MWT	MI	JE	%	MWT	MI	JE	%	MWT	MI	JE	%	MWT	MI	JE	%
1	bior2.4	1.31	3.24	40.24	bior3.1	1.06	3.63	29.32	db1	0.88	2.59	33.97	db1	0.88	2.59	33.97
2	bior3.3	1.33	2.99	44.59	bior2.8	1.45	5.12	28.40	db1	1.06	2.71	39.01	db1	1.06	2.71	39.01
3	db1	0.78	1.34	58.62	bior2.8	0.85	4.23	20.08	db1	0.78	1.34	58.62	db1	0.78	1.34	58.62
5	db1	1.43	3.07	46.55	bior4.4	1.39	5.04	27.49	db1	1.43	3.07	46.55	db1	1.43	3.07	46.55
7	bior2.2	1.64	5.82	28.27	bior3.1	1.71	6.80	25.16	bior2.2	1.64	5.82	28.27	bior2.2	1.64	5.82	28.27
10	db1	1.35	3.08	43.88	bior3.1	1.46	4.13	35.42	db1	1.35	3.08	43.88	db1	1.35	3.08	43.88
11	db6	2.72	6.40	42.53	bior3.1	2.84	7.16	39.74	db6	2.72	6.40	42.53	db10	2.72	6.58	41.39
Average				43.53				29.37								41.67

7. Conclusions

In this study, we have proposed the Information Quality Ratio (IQR) for MWT selection. The experiment has several interesting results as follows: Determining decomposition level is a fundamental step in wavelet transform because improper decomposition level will lead to not optimum signal reconstruction that causes a signal defect. It has to become caution for researchers and practitioners to determine the appropriate level of wavelet decomposition. Moreover, IQR has successfully determined the best-suited MWT for e-nose signals in the beef quality classification task. Each signal has its own characteristics, so it certainly has different MWT than others. According to the experimental results, IQR has better sensitivity to detect the changes of signal structure than MSE and correlation coefficient. Furthermore, IQR based MWTs have better capabilities to keep essential information than SNR, MSE, and correlation coefficient based MWTs. Different from the MSE and correlation coefficient that emphasize on the morphological similarity and SNR which is based on the signal to noise power, this new metric is focused on how good wavelet transform can reconstruct the signal without losing essential information.

References

- Z. Ali, W.T.O. Hare, B.J. Theaker, Detection of bacterial contaminated milk by means of a quartz crystal microbalance based electronic nose, *J. Therm. Anal. 71* (2003) 155–161.
- S. Ampuero, T. Zesiger, V. Gustafsson, A. Lunden, J.O. Bosset, Determination of trimethylamine in milk using an MS based electronic Nose, *Eur. Food Res. Technol.* 214 (2002) 163–167. <http://dx.doi.org/10.1007/s00217-001-0463-0>.
- S. Borah, E.L. Hines, M.S. Leeson, D.D. Iliescu, M. Bhuyan, J.W. Gardner, Neural network based electronic nose for classification of tea aroma, *Sens. Instrum. Food Qual. Saf.* 2 (2008) 7–14. <http://dx.doi.org/10.1007/s11694-007-9028-7>.
- S. Omatu, M. Yano, E-nose system by using neural networks, *Neurocomputing* 172 (2016) 394–398. <http://dx.doi.org/10.1016/j.neucom.2015.03.101>.
- S. G??ney, A. Atasoy, Study of fish species discrimination via electronic nose, *Comput. Electron. Agric.* 119 (2015) 83–91. <http://dx.doi.org/10.1016/j.compag.2015.10.005>.
- S. Kiani, S. Minaei, M. Ghasemi-Varnamkhasti, A portable electronic nose as an expert system for aroma-based classification of saffron, *Chemom. Intell. Lab. Syst.* (2016). <http://dx.doi.org/10.1016/j.chemolab.2016.05.013>.
- Radi, S. Ciptohadijoyo, W.S. Litananda, M. Rivai, M.H. Purnomo, Electronic nose based on partition column integrated with gas sensor for fruit identification and classification, *Comput. Electron. Agric.* 121 (2016) 429–435. <http://dx.doi.org/10.1016/j.compag.2015.11.013>.
- O.S. Papadopoulou, E.Z. Panagou, F.R. Mohareb, G.J.E. Nychas, Sensory and microbiological quality assessment of beef fillets using a portable electronic nose in tandem with support vector machine analysis, *Food Res. Int.* 50 (2013) 241–249. <http://dx.doi.org/10.1016/j.foodres.2012.10.020>.
- S.A. Abdallah, L.A. Al-shatti, A.F. Alhajraf, N. Al-hammad, B. Al-awadi, Detect. foodborne Bact. beef. Appl. Electron. nose (2013) 1–9. [10.1186%2F2193-1801-2-687](http://dx.doi.org/10.1186%2F2193-1801-2-687).
- S.A. Abdallah, L.A. Al-shatti, A.F. Alhajraf, N. Al-hammad, B. Al-awadi, The detection of foodborne bacteria on beef: the application of the electronic nose, 2013, pp. 1–9. <http://dx.doi.org/10.1186%2F2193-1801-2-687>.
- S. Balasubramanian, C.M. Logue, M. Marchello, Spoilage Identification of Beef Using an Electronic Nose System, *Trans. ASAE* 47 (2004) 1625–1633. <http://dx.doi.org/10.13031/2013.17593>.
- M. Ghasemi-Varnamkhasti, S.S. Mohtasebi, M. Siadat, S. Balasubramanian, Meat Quality Assessment by Electronic Nose (Machine Olfaction Technology), *Sensors* 9 (2009) 6058–6083. <http://dx.doi.org/10.3390/s90806058>.
- V.Y. Musatov, V.V. Sysyov, M. Sommer, I. Kiselev, Assessment of meat freshness with metal oxide sensor microarray electronic nose: a practical approach, *Sens. Actuators B: Chem.* 144 (2010) 99–103. <http://dx.doi.org/10.1016/j.snb.2009.10.040>.
- N. El Barbri, E. Llobet, N. El Bari, X. Correig, B. Bouchikki, Electronic Nose Based on Metal Oxide Semiconductor Sensors as an Alternative Technique for the Spoilage Classification of Red Meat, *Sensors* 8 (2008) 142–156. <http://dx.doi.org/10.3390/s8010142>.
- A.K. Bag, B. Tudu, Rough Set Based Classification on Electronic Nose Data for BlackTea Application, (n.d.), pp. 23–31.
- P. Saha, S. Ghorai, B. Tudu, R. Bandyopadhyay, N. Bhattacharyya, Optimization of sensor array in electronic nose by combinational feature selection method, 2012, in: *Proceedings of the Sixth International Conference on Sensing Technology (ICST)*, 2012, pp. 341–346. doi:10.1109/ICST.2012.6461698
- Z. Xu, X. Shi, S. Lu, Integrated sensor array optimization with statistical evaluation, *Sens. Actuators, B: Chem.* 149 (2010) 239–244. <http://dx.doi.org/10.1016/j.snb.2010.05.038>.
- X. Hong, J. Wang, G. Qi, Comparison of spectral clustering, K-clustering and hierarchical clustering on e-nose datasets: application to the recognition of material freshness, adulteration levels and pretreatment approaches for tomato juices, *Chemom. Intell. Lab. Syst.* 133 (2014) 17–24. <http://dx.doi.org/10.1016/j.chemolab.2014.01.017>.
- X. Hong, J. Wang, G. Qi, Comparison of semi-supervised and supervised approaches for classification of e-nose datasets: case studies of tomato juices, *Chemom. Intell. Lab. Syst.* 146 (2015) 457–463. <http://dx.doi.org/10.1016/j.chemolab.2015.07.001>.
- W. Guo, F. Gan, H. Kong, J. Wu, Signal model of electronic noses with metal oxide semiconductor, *Chemom. Intell. Lab. Syst.* 143 (2015) 130–135. <http://dx.doi.org/10.1016/j.chemolab.2015.02.021>.
- F. Tian, S.X. Yang, K. Dong, Circuit and noise analysis of odorant gas sensors in an E-Nose, *Sensors* 5 (2005) 85–96. <http://dx.doi.org/10.3390/s010085>.
- D.R. Wijaya, R. Sarno, Mobile electronic nose architecture for beef quality detection based on internet of things technology, in: *Bandungpp*. 655–663. <http://www.globalilluminators.org/wp-content/uploads/2015/05/GTAR-15-331.pdf>, 2015.
- Najam ul Hasan, N. Ejaz, W. Ejaz, H.S. Kim, Meat and fish freshness inspection system based on odor sensing, *Sens. (Switz.)* 12 (2012) 15542–15557. <http://dx.doi.org/10.3390/s121115542>.
- V.S. Kodogiannis, A. Alshejari, A Fuzzy-Wavelet Neural Network Model for the Detection of Meat Spoilage using an Electronic Nose, in: *IEEE World Congress on Computational Intelligence (IEEE WCCI)*, IEEE, 2016.
- F. Mohareb, O. Papadopoulou, E. Panagou, G.-J. Nychas, C. Bessant, Ensemble-based support vector machine classifiers as an efficient tool for quality assessment of beef fillets from electronic nose data, *Anal. Methods* 8 (2016) 3711–3721. <http://dx.doi.org/10.1039/c6ay00147e>.
- A.F. Egan, I.J. Eustace, B.J. Shay, Meat packaging - maintaining the quality and prolonging the storage life of chilled beef, pork and lamb, in: *Proceedings of Industry Day: Part of the 34th International Congress of Meat Science and Technology*, Brisbane, 1988, pp. 68–75.
- L. Pasti, B. Walczak, D.L. Massart, P. Reschiglian, Optimization of signal denoising in discrete wavelet transform, *Chemom. Intell. Lab. Syst.* 48 (1999) 21–34. [http://dx.doi.org/10.1016/S0169-7439\(99\)00002-7](http://dx.doi.org/10.1016/S0169-7439(99)00002-7).
- J.A. Sáez, M. Galar, J. Luengo, F. Herrera, Analyzing the presence of noise in multi-class problems: alleviating its influence with the One-vs-One decomposition, *Knowl. Inf. Syst.* 38 (2014) 179–206. <http://dx.doi.org/10.1007/s10115-012-0570-1>.
- X. Zhu, X. Wu, Class noise vs. attribute noise: a quantitative study, *Artif. Intell. Rev.* 22 (2004) 177–210. <http://dx.doi.org/10.1007/s10462-004-0751-8>.
- J. Feng, F. Tian, J. Yan, Q. He, Y. Shen, L. Pan, A background elimination method based on wavelet transform in wound infection detection by electronic nose, *Sens. Actuators, B: Chem.* 157 (2011) 395–400. <http://dx.doi.org/10.1016/j.snb.2011.04.069>.
- Y. Chompusri, K. Dejhan, S. Yimman, Mother Wavelet Selecting Method for Selective Mapping Technique ECG Compression, in: *2012 Proceedings of the 9th International Conference on Electrical Engineering/Electronics, Computer,*

- Telecommunications and Information Technology (ECTI-CON), IEEE, Phetchaburi, 2012: pp. 1–4. <http://dx.doi.org/10.1109/ECTICon.2012.6254213>.
- [32] U.Seljuq, F.Himayun, H.Rasheed, Selection of an optimal mother wavelet basis function for ECG signal denoising, in: Proceedings of the 17th IEEE International Multi Topic Conference 2014., 2014, pp. 26–30. <http://dx.doi.org/10.1109/INMIC.2014.7096905>.
- [33] N.K.Al-qazzaz, S.Ali, S.A.Ahmad, S.Islam, Selection of Mother Wavelets Thresholding Methods in Denoising Multi-channel EEG Signals during Working Memory Task, in: 2014 IEEE Conference on Biomedical Engineering and Sciences (IECBES), IEEE, Kuala Lumpur, 2014: pp. 8–10. <http://dx.doi.org/10.1109/IECBES.2014.7047488>.
- [34] N. Al-Qazzaz, S. Hamid Bin Mohd Ali, S. Ahmad, M. Islam, J. Escudero, Selection of mother wavelet functions for multi-channel EEG signal analysis during a working memory task, *Sensors*. 15 (2015) 29015–29035. <http://dx.doi.org/10.3390/s151129015>.
- [35] T. Gandhi, B.K. Panigrahi, S. Anand, A comparative study of wavelet families for EEG signal classification, *Neurocomputing*. 74 (2011) 3051–3057. <http://dx.doi.org/10.1016/j.neucom.2011.04.029>.
- [36] D. Wang, D. Miao, C. Xie, Best basis-based wavelet packet entropy feature extraction and hierarchical EEG classification for epileptic detection, *Expert Syst. Appl.* 38 (2011) 14314–14320. <http://dx.doi.org/10.1016/j.eswa.2011.05.096>.
- [37] J. Rafiee, M.A. Rafiee, N. Prause, M.P. Schoen, Wavelet basis functions in biomedical signal processing, *Expert Syst. Appl.* 38 (2011) 6190–6201. <http://dx.doi.org/10.1016/j.eswa.2010.11.050>.
- [38] F. Adamo, G. Andria, F. Attivissimo, A.M.L. Lanzolla, M. Spadavecchia, A comparative study on mother wavelet selection in ultrasound image denoising, *Meas.: J. Int. Meas. Confed.* 46 (2013) 2447–2456. <http://dx.doi.org/10.1016/j.measurement.2013.04.064>.
- [39] K.Ferroudji, N.Benoudjit, M.Bahaz, aBouakaz, Selection of a suitable mother wavelet for microemboli classification using SVM and RF signals, 2012 in: Proceedings of the 24th International Conference on Microelectronics (ICM). 1, 2012, pp. 1–4. <http://dx.doi.org/10.1109/ICM.2012.6471382>.
- [40] R. Maheswaran, R. Khosa, Comparative study of different wavelets for hydrologic forecasting, *Comput. Geosci.* 46 (2012) 284–295. <http://dx.doi.org/10.1016/j.cageo.2011.12.015>.
- [41] M. Shoaib, A.Y. Shamseldin, B.W. Melville, Comparative study of different wavelet based neural network models for rainfall-runoff modeling, *J. Hydrol.* 515 (2014) 47–58. <http://dx.doi.org/10.1016/j.jhydrol.2014.04.055>.
- [42] a I.Megahed, a M.Moussa, H.B.Elrefaie, Y.M.Marghany, Selection of a suitable mother wavelet for analyzing power system fault transients, IEEE Power and Energy Society 2008 General Meeting: Conversion and Delivery of Electrical Energy in the 21st Century, PES, 2008, pp. 1–7. <http://dx.doi.org/10.1109/PES.2008.4596367>.
- [43] J. Saraswathy, M. Hariharan, T. Nadarajaw, W. Khairunizam, S. Yaacob, Optimal selection of mother wavelet for accurate infant cry classification, *Australas. Phys. Eng. Sci. Med.* 37 (2014) 439–456. <http://dx.doi.org/10.1007/s13246-014-0264-y>.
- [44] H. He, Y. Tan, Y. Wang, Optimal base wavelet selection for ECG noise reduction using a comprehensive entropy criterion, *Entropy*. 17 (2015) 6093–6109. <http://dx.doi.org/10.3390/e17096093>.
- [45] R. Yan, R.X. Gao, Base wavelet selection for bearing vibration signal analysis, *Int. J. Wavelets, Multiresolution Inf. Process.* 7 (2009) 411–426.
- [46] R.X. Gao, R. Yan, *Wavelets: theory and Applications for Manufacturing*, Springer, New York, 2011. <http://dx.doi.org/10.1007/978>.
- [47] E. Borch, M.L. Kant-Muermans, Y. Blixt, Bacterial spoilage of meat and cured meat products, *Int. J. Food Microbiol.* 33 (1996) 103–120. [http://dx.doi.org/10.1016/0168-1605\(96\)01135-X](http://dx.doi.org/10.1016/0168-1605(96)01135-X).
- [48] J.P. Harley, L.M. Prescott, *Laboratory Exercise in Microbiology*, 5th ed., McGraw-Hill, 2002. <http://dx.doi.org/10.1007/s13398-014-0173-7.2>.
- [49] D.R. Wijaya, R. Sarno, E. Zulaika, Sensor array optimization for mobile electronic nose: wavelet transform and filter based feature selection approach, *Int. Rev. Comput. Softw.* 11 (2016).
- [50] X. Liu, S. Cheng, H. Liu, S. Hu, D. Zhang, H. Ning, I. Engineering, A survey on gas sensing technology, *Sens. (Switz.)* 12 (2012) 9635–9665. <http://dx.doi.org/10.3390/s120709635>.
- [51] G. Brown, A. Pocock, M.-J. Zhao, M. Lujan, Conditional likelihood maximisation: a unifying framework for mutual information feature selection, *J. Mach. Learn. Res.* 13 (2012) 27–66. <http://dx.doi.org/10.1016/j.patcog.2015.11.007>.
- [52] J.R. Vergara, P.A. Est?vez, A review of feature selection methods based on mutual information, *Neural Comput. Appl.* 24 (2014) 175–186. <http://dx.doi.org/10.1007/s00521-013-1368-0>.
- [53] Y. Saeys, I. Inza, P. Larranaga, A review of feature selection techniques in bioinformatics, *Bioinformatics*. 23 (2007) 2507–2517. <http://dx.doi.org/10.1093/bioinformatics/btm344>.
- [54] B.Senliol, G.Gulgezen, L.Yu, Z.Cataltepe, Fast Correlation Based Filter (FCBF) with a different search strategy, 2008 in: Proceedings of the 23rd International Symposium on Computer and Information Sciences, ISCIS 2008., 2008, pp. 0–3. <http://dx.doi.org/10.1109/ISCIS.2008.4717949>.
- [55] L.Yu, H.Liu, Feature Selection for High-Dimensional Data: A Fast Correlation-Based Filter Solution, in: Proceedings of the Twentieth International Conference on Machine Learning (ICML-2003), AAAI, Washington DC, 2003: pp. 856–863.
- [56] Y. Shin, D. Kwiatkowski, P. Schmidt, P.C.B. Phillips, Testing the Null Hypothesis of Stationarity Against the Alternative of a Unit Root: how Sure Are We That Economic Time Series Are Nonstationary?, *J. Econ.* 54 (1992) 159–178. [http://dx.doi.org/10.1016/0304-4076\(92\)90104-Y](http://dx.doi.org/10.1016/0304-4076(92)90104-Y).
- [57] S. Saraçlı, N. Dogan, I. Dogan, Comparison of hierarchical cluster analysis methods by cophenetic correlation, *J. Inequalities Appl.* 1 (2013) 1–8. <http://dx.doi.org/10.1186/1029-242X-2013-203>.
- [58] P.F. Jia, F.C. Tian, S. Fan, Q.H. He, J.W. Feng, S.X. Yang, A novel sensor array and classifier optimization method of electronic nose based on enhanced quantum-behaved particle swarm optimization, *Sens. Rev.* 34 (2014) 304–311. <http://dx.doi.org/10.1108/Sr-02-2013-630>.
- [59] P.M. Szcz?wka, a Szczurek, B.W. Licznarski, On reliability of neural network sensitivity analysis applied for sensor array optimization, *Sens. Actuators B: Chem.* 157 (2011) 298–303. <http://dx.doi.org/10.1016/j.snb.2011.03.066>.
- [60] Z. Xu, S. Lu, Multi-objective optimization of sensor array using genetic algorithm, *Sens. Actuators, B: Chem.* 160 (2011) 278–286. <http://dx.doi.org/10.1016/j.snb.2011.07.048>.